J Physiol 586.19 (2008) pp 4721–4733

The Journal of Physiology

Alteration in left ventricular normal and shear strains evaluated by 2D-strain echocardiography in the athlete's heart

S. Nottin[1], G. Doucende[1], I. Schuster-Beck[2], M. Dauzat[2] and P. Obert[1]

[1]*EA 4278, Physiology and Physiopathology of Cardiovascular Adaptations to Exercise, Faculty of Sciences, Avignon University, Avignon, France*
[2]*EA 2992, Cardiovascular Research Laboratory, Faculty of Medicine, Montpellier I University, Nîmes, France*

The contraction of cardiomyocytes induces a systolic increase in left ventricular (LV) normal (radial, circumferential and longitudinal) and shear strains, whose functional consequences have not been evaluated, so far, in athletes. We used 2D ultrasound speckle tracking imaging (STI) to evaluate LV regional strain in high-level cyclists compared to sedentary controls. Sixteen male elite cyclists and 23 sedentary controls underwent conventional, tissue Doppler, and STI echocardiography at rest. We assessed LV long and short axis normal strains and shear strains. We evaluated circumferential–longitudinal shear strain from LV torsion, and circumferential–radial shear strain from the difference between subendocardial and subepicardial torsion. Apical radial strain (42.7 ± 10.5% *versus* 52.2 ± 14.3%, $P < 0.05$) and LV torsion (6.0 ± 1.8 deg *versus* 9.2 ± 3.2 deg, $P < 0.01$) were lower in cyclists than in controls, respectively. Rotations and torsion were higher in the subendocardial than in the subepicardial region in sedentary controls, but not in cyclists. Haemodynamic and tissue Doppler based indexes of global LV diastolic and systolic functions were not different between cyclists and controls. Athlete's heart is associated with specific LV adaptation including lower apical strain and lower myocardial shear strains, with no change in global LV diastolic and systolic function. These mechanical alterations could improve the cardiovascular adjustments to exercise by increasing the radial strain and torsional (and thus untwisting) response to exercise, a key element of diastolic filling and thus of cardiac performance in athletes.

(Received 5 May 2008; accepted after revision 31 July 2008; first published online 7 August 2008)
Corresponding author S. Nottin: Physiologie et Physiopathologie Adaptations Cardiovasculaires à l'Exercice, 33, Rue Louis Pasteur, 84000 Avignon, France. Email: stephane.nottin@univ-avignon.fr

During systole, contraction of cardiomyocytes induces myocardial normal strains, including longitudinal shortening (from base to apex), circumferential shortening (perpendicular to radial and to the longitudinal axis) and radial thinning (perpendicular to epicardium and to the longitudinal axis) (Moore *et al.* 2000). Each strain can be defined as the fractional change in length compared to its end-diastolic length. Moreover, due to the helically orientated myofibres (Torrent-Guasp *et al.* 2001), following right-handed and left-handed helical pathways in the subendocardial and subepicardial layers, respectively (Greenbaum *et al.* 1981), contraction also induces shear strains (i.e. transmural strains) within the myocardium (Rosen *et al.* 2004) including longitudinal–radial, circumferential–radial and circumferential–longitudinal components. Magnetic resonance imaging (MRI) studies have provided detailed insight into myocardial relaxation mechanisms and shown that, during diastole, shear strains decrease before normal strains (Rosen *et al.* 2004). This 'elastic recoil' (Notomi *et al.* 2006) causes the rapid reduction of left ventricular (LV) pressure that leads in turn to mitral valve opening and early filling (Dong *et al.* 2001; Notomi *et al.* 2008). Insight into myocardial normal and shear strains is therefore crucial for a better understanding of the complex LV mechanics that underlies LV function in the human heart.

The athlete's heart is a LV adaptation to long-term intensive endurance training characterized by an increase in chamber size, wall thickness and mass (Pelliccia *et al.* 1991). Most echocardiographic studies have evaluated ejection fraction and transmitral flow velocities to search for a relationship between cardiac hypertrophy and LV systolic and diastolic function (Pluim *et al.* 2000; Fagard, 2003). However, these haemodynamic variables do not provide any direct information about the myocardium motion and function. The tissue Doppler imaging (TDI) technique has been introduced to overcome this limitation

DOI: 10.1113/jphysiol.2008.156323

(Caso *et al.* 2000; Schmidt-Trucksäss *et al.* 2001; Nottin *et al.* 2004; Saghir *et al.* 2007). However, as TDI measures velocities relative to the direction of the ultrasound beam, it yields only the longitudinal component of LV mechanics. To the best of our knowledge, and despite their relevance in the comprehension of LV function, normal and shear strains have never been investigated to date in the athlete's heart. Sympathetic activity (Maruo *et al.* 2007; Notomi *et al.* 2008), by its inotropic and lusitropic effects, and also LV dimensions and loading conditions (Moon *et al.* 1994; MacGowan *et al.* 1996) are important determinants of normal as well as shear strains. Since all these parameters differ at rest between athletes and sedentary individuals, alterations in normal and shear strains might be expected in the athlete's heart. The non-invasive evaluation of LV strains has been so far limited to tagged MRI, which is not widely available, and cannot be used in routine clinical practice. Recently, the development of 2D ultrasound speckle tracking imaging (STI) has allowed the angle dependence of TDI to be overcome and LV normal strains to be non-invasively evaluated (Amundsen *et al.* 2006). Moreover, STI has the capability to assess LV torsion (Helle-Valle *et al.* 2005), and to distinguish torsion of the subendocardial and subepicardial layers of the myocardium (Hui *et al.* 2007), thus providing information on the circumferential–longitudinal and circumferential–radial components of shear strains, respectively. In the present study, we used STI to evaluate LV normal and shear strains underlying the global LV function in the athlete's heart.

Methods

Study population

We evaluated 16 male elite cyclists and 23 age-matched sedentary controls. The elite cyclists participated in national cross-country cycling events and had been training 12.4 ± 3.6 hours per week for 11.0 ± 4.8 years, whereas none of the sedentary men reported regular training habits. All subjects underwent conventional and colour tissue Doppler echocardiography. None of them had any clinical or historical evidence of cardiovascular disease or arterial hypertension. A biometric evaluation including assessment of body fat mass by skin-fold thickness measurements was performed on all subjects (Durnin & Rahaman, 1967). This study received approval from the local ethics committee and written informed consent was obtained from all subjects. The study conformed with the *Declaration of Helsinki*.

Echocardiographic image acquisition

Images were obtained in the left lateral decubitus position after a 15 min resting period using a commercially available system (Vivid I, GE Healthcare, Horten, Norway) with a 3.5 MHz sector scanning electronic transducer. Gains and filters were adjusted carefully to eliminate background noise and allow for a clear tissue signal. Two-dimensional greyscale harmonic images were obtained at a rate of 60–75 frames s^{-1}, and separate harmonic colour tissue velocity images were saved at a rate of 120–140 frames s^{-1}, depending on both the depth and the sector width. Images were acquired in cine loops triggered to the QRS complex and saved digitally for subsequent off-line analysis with dedicated software (EchoPac 6.0, GE Healthcare, Horten, Norway). Measurements in athletes and in controls were obtained in a blind fashion.

Standard parameters

Standard echocardiograms consisted of two-dimensional, M-Mode and Doppler blood flow measurements. M-Mode measurements were obtained, according to the recommendations of the American Society of Echocardiography, in the parasternal long-axis view (Sahn *et al.* 1978). LV mass was calculated according to the Penn convention (Devereux *et al.* 1986). Pulsed Doppler LV inflow recordings, including early (E) and atual (A) waves, were performed in the apical four-chamber view, with the sample volume at the tip level of the mitral valves. Stroke volume was calculated as the product of the aortic root area and the integral of the aortic blood flow velocity recorded from a five-chamber view. Cardiac output was calculated as the product of stroke volume and heart rate and systemic vascular resistances as the ratio of mean arterial pressures and cardiac output.

Tissue Doppler imaging

Color cine loops were recorded in the apical two-, three- and four-chamber views for subsequent off-line tissue Doppler analysis. We assessed wall motion velocities at the mitral annulus level on the septal, lateral, inferior, anterior, antero-septal and posterior walls. Peak myocardial systolic velocity (S_m) and early (E_m) and atial (A_m) diastolic velocities were derived for each wall. The peak myocardial acceleration during isovolumic contraction (A_{IVC}), recorded at the level of the lateral wall of the mitral annulus, was also used as an index of global LV contractility (Hashimoto *et al.* 2005). The E/E_m ratio, recorded at the level of the lateral wall of the mitral annulus, was used as an index of LV filling pressure (Nagueh *et al.* 1997).

Speckle tracking imaging

The computer automatically selected suitable stable objects for tracking and then searched for them in the next frame using the sum of absolute difference

algorithm (Leitman *et al.* 2004). After manually tracing the endocardial border on the end-systolic frame of the 2-D sequence, the software automatically tracked myocardial motion, creating six equidistant speckle tracking regions of interest in each image. Whenever the software signalled poor tracking efficiency, the observer readjusted the endocardial trace line and/or the region of interest width until a better tracking score could be obtained.

We evaluated three normal strains (Fig. 1), namely longitudinal and circumferential shortening/elongation and radial thickening/thinning, and two shear strains, namely shear in the circumferential and longitudinal plane and in the circumferential and radial plane. LV longitudinal strain and strain rate (SR) analysis was performed using an apical four-chamber view. Peak global longitudinal SR during the isovolumic relaxation period (SR_{IVR}), a preload independent index of LV relaxation, was calculated as proposed by Wang *et al.* (2007). Radial and circumferential strain and SR analysis was performed on short-axis views. LV rotations, resulting from circumferential–longitudinal shear strains inside the myocardium, were calculated from basal and apical short axis views. Care was taken to ensure that the basal short-axis plane contained the mitral valve, and that the apical plane was acquired distally to the papillary muscle. The width of the region of interest was adjusted first, to include the entire myocardium. To obtain information on circumferential–radial strains, the region of interest was then set to include only the subendocardial and subepicardial layers in order to evaluate the difference in torsion between the inner and outer layers (Hui *et al.* 2007). Basal and apical rotation of the entire myocardium and subendocardial and subepicardial layers were analysed in 12 subjects blindly on two separate days by an experienced cardiologist in order to assess intraobserver reproducibility. Since the reproducibility was good, only data on the first assessment were presented in the present study (myocardium – C.V.: 5.4–11.9%; R^2: 0.97–0.99; subendocardial layer – C.V.: 8.1–9.1%; R^2: 0.92–0.99; subepicardial layer – C.V.: 13.3–13.9%; R^2: 0.89–0.92).

In order to assess the dynamics of global LV twist and its relation to radial displacement throughout the cardiac cycle, we constructed twist-displacement loops (Nakai *et al.* 2006). Averaged radial displacement data from six segments in basal and in apical short-axis planes were summed and divided by 2 to obtain the mean value of radial displacement throughout the cardiac cycle. Twist-displacement loops were constructed for each subject. To create average twist-displacement loop in each

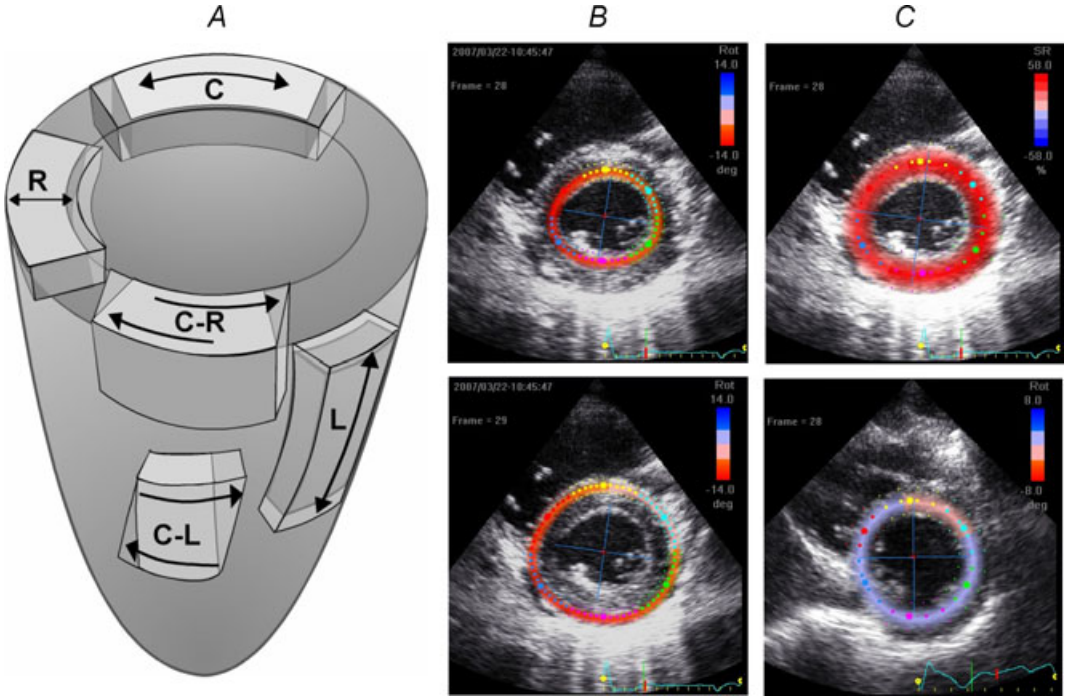

Figure 1 Directions of normal and shear strains
A, illustration of the systolic strains evaluated in the study: longitudinal (L), radial and circumferential (C) strains; circumferential–radial (C-R) and circumferential–longitudinal (C-L) shear strains. *B*, adjustment of the region of interest on both subendocardial and subepicardial layers in order to evaluate the difference of torsion between the inner and outer layers. *C*, adjustment of the region of interest on the entire myocardium to assess both LV basal and apical rotations.

group, the time sequence was normalized to the percentage of systolic duration.

All data were exported to a spreadsheet program (Microsoft Excel) to calculate LV torsion and torsion rate. To adjust all strain parameters for intersubject differences in heart rate, the time sequence was also normalized to the percentage of systolic duration (i.e. t was 100% at end systole). Spreadsheet calculation allowed the detection of peak systolic and diastolic SR, the peak of LV twist and untwist rates, and the time to these peaks.

Statistical analysis

The statistical analysis was performed with Statview 5.0 (SAS Institute, Cary, NC, USA). Data were expressed as means ± S.D. Analysis of variance was used to compare each variable between the two groups. The significance of variation in torsion at different locations was determined by a two-way analysis of variance (group × location). Simple linear regression analyses between HR and LV radial strain, strain rate, torsion, twisting and untwisting rate were performed. Statistical significance was assessed when $P < 0.05$.

Table 1. Standard echocardiography

	Controls	Cyclists
Morphological parameters		
LV end-diastolic diameter (mm)	49.5 ± 3.8	56.8 ± 3.1***
LV end-systolic diameter (mm)	30.4 ± 3.6	36.2 ± 3.5***
Septal wall thickness (mm)	11.0 ± 1.4	12.8 ± 1.3***
Posterior wall thickness (mm)	6.8 ± 0.8	8.1 ± 1.2**
LV mass (g)	154 ± 24	238 ± 29***
Ratio wall thickness/ end-diastolic diameter	0.36 ± 0.05	0.36 ± 0.05
Global diastolic function		
Peak E velocity (cm s^{-1})	80.2 ± 7.8	81.9 ± 7.7
Peak A velocity (cm s^{-1})	49.5 ± 8.4	42.8 ± 7.0*
Peak E/A ratio	1.70 ± 0.37	1.95 ± 0.30*
Global systolic function		
Fractional shortening (%)	38.6 ± 4.6	36.3 ± 4.1
Heart rate (beat min^{-1})	70 ± 10	56 ± 7***
Stroke volume (ml)	75.9 ± 11.4	100.0 ± 11.3***
Cardiac output (l min^{-1})	5.3 ± 1.1	5.6 ± 1.0
Arterial pressures		
Systolic (mmHg)	135 ± 15	127 ± 8
Diastolic (mmHg)	70 ± 9	69 ± 9
Systemic vascular resistances (A.U.)	17.6 ± 3.2	16.1 ± 3.1

Significant differences: *$P < 0.05$; **$P < 0.01$; ***$P < 0.001$.

Results

Biometric data

There were no differences in age (24.6 ± 4.6 *versus* 22.6 ± 5.4 year), height (179.1 ± 6.5 *versus* 179.0 ± 6.3 cm) and body mass (71.5 ± 5.8 *versus* 73.1 ± 9.7 kg) between controls and cyclists, respectively. The cyclists exhibited a lower percentage of body fat mass than controls (12.6 ± 2.4 *versus* 16.8 ± 4.5%; $P < 0.001$).

Standard echocardiography and TDI

Elite cyclists exhibited a marked LV hypertrophy on account of increased cavity dimension and wall thickness (Table 1). However, the ratio of wall thickness to LV radius was similar in controls and cyclists.

Haemodynamic parameters of LV global diastolic and systolic functions are presented in Table 1. Cyclists had higher stroke volume and lower heart rate than controls. There was no difference in cardiac output, systemic vascular resistances, or fractional shortening between the two groups. The cyclists and controls showed also similar mean (i.e. mean of the 6 walls) peak S_m (7.6 ± 0.8 *versus* 8.0 ± 0.8 cm s^{-1}, respectively) and A_{IVC} (184 ± 35 *versus* 204 ± 63 cm s^{-2}, respectively). Cyclists had similar peak E, but lower peak A than controls, resulting in higher E/A ratio in the former. There was no difference in mean peak E_m between the two groups (11.9 ± 1.8 *versus* 11.5 ± 1.8 cm s^{-1}, respectively). Mean peak A_m was non-significantly lower (4.6 ± 0.8 *versus* 5.2 ± 1.9 cm s^{-1}), and the E/lateral E_m ratio was similar (6.2 ± 1.0 *versus* 5.7 ± 0.7) in the cyclists and controls, respectively.

Regional LV strains

Patterns of longitudinal, radial and circumferential strains during the cardiac cycle are reported in Fig. 2. Peak systolic and diastolic SR and their respective time to peak (expressed as percentage of systole duration) are presented in Table 2. Longitudinal strains (−19.2 ± 1.9% *versus* −19.5 ± 2.2%), systolic and diastolic peak and time to peak longitudinal SR (Table 2) and longitudinal SR_{IVR} (0.19 ± 0.11 s^{-1} *versus* 0.22 ± 0.09 s^{-1}) did not differ between the cyclists and controls, respectively. Similar results were obtained for peak circumferential strains (−16.0 ± 3.5% *versus* −16.2 ± 3.4% at the basal level and −18.1 ± 2.5% *versus* −18.6 ± 4.1% at the apical level) as well as systolic and diastolic peak and time to peak circumferential SR. However, peak apical radial strains were lower in cyclists than in controls (42.7 ± 10.5% *versus* 52.2 ± 14.3%, $P < 0.05$). Peak apical radial SR was also lower in the cyclists during systole but not during diastole. HR correlated with peak apical radial strains ($P < 0.01$) and peak apical radial SR during systole ($P < 0.05$) (Fig. 3). Peak basal radial strains (41.7 ± 11.9%

versus 41.5 ± 14.4%), and their respective peak and time to peak SR were not different in cyclists and controls, respectively.

Basal and apical rotations and LV torsion are presented in Fig. 4. As viewed from the apex, positive values represent counterclockwise rotation and negative values clockwise rotation. In both groups, similar patterns of LV rotations and torsion were obtained. LV torsion was produced by counterclockwise apical rotation and clockwise basal rotation. At aortic valve closure (AVC), there was no significant difference in basal rotation between the cyclists and controls (−5.2 ± 2.4% *versus* −4.8 ± 3.2%, respectively). However, the cyclists showed lower apical rotation (1.7 ± 1.9% *versus* 4.0 ± 2.9%, $P < 0.05$) and lower LV torsion (6.0 ± 1.8% *versus* 9.2 ± 3.2%, $P < 0.01$) than controls, respectively. Rotational rate at the apical

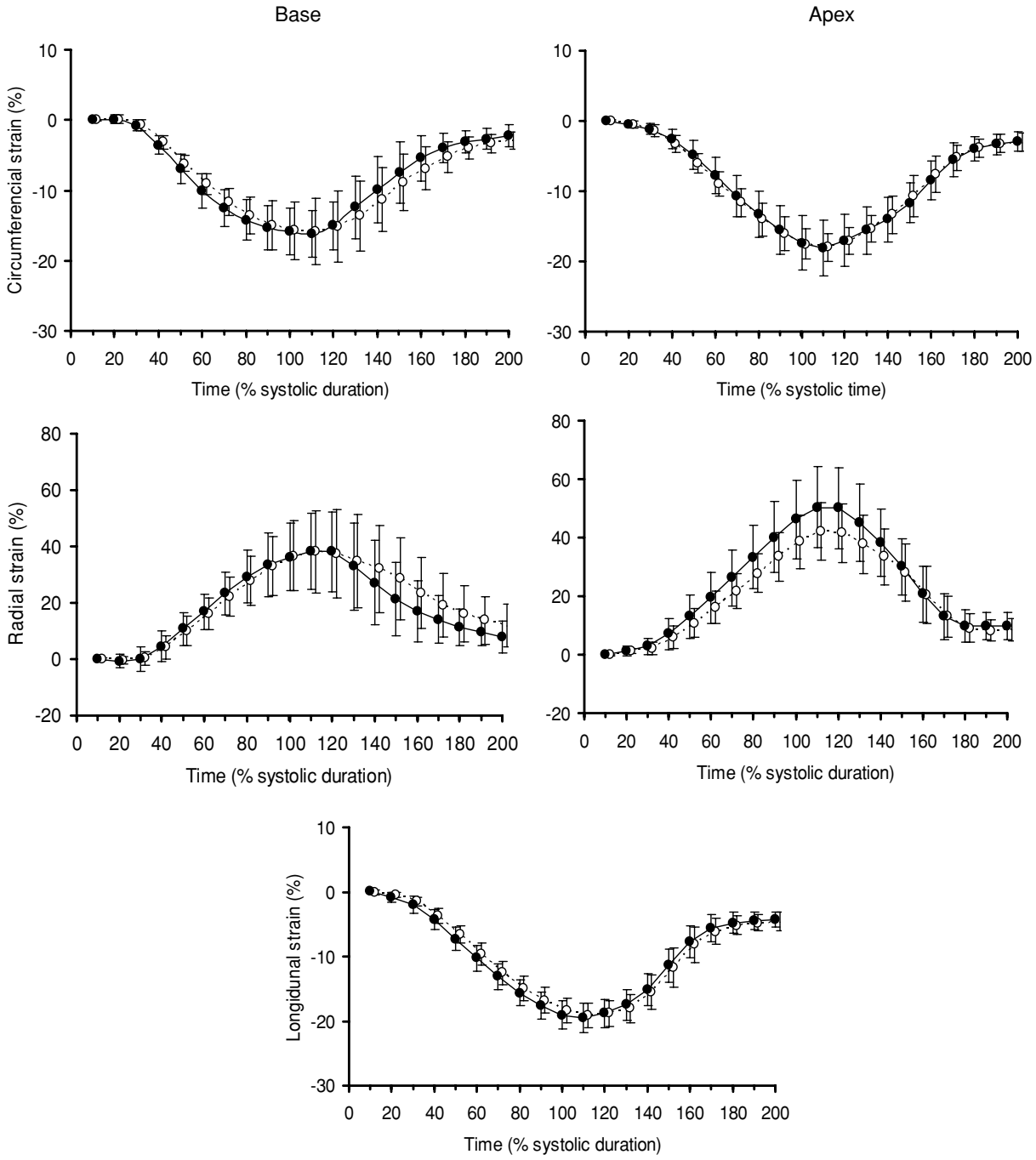

Figure 2. LV basal and apical circumferential and radial strains and LV longitudinal strains in sedentary subjects (●) and cyclists (○)

Table 2. Peak and time to peak strain rates during systole and diastole

	Controls		Cyclists	
	Peak	Time to peak	Peak	Time to peak
Systole				
Longitudinal SR (s^{-1})	-1.08 ± 0.15	45 ± 9	-1.01 ± 0.13	49 ± 5
Radial SR (s^{-1})				
Basal level	1.64 ± 0.35	41 ± 14	1.39 ± 0.33*	41 ± 12
Apical level	1.59 ± 0.33	47 ± 17	1.33 ± 0.22*	57 ± 14
Circumferential SR (s^{-1})				
Basal level	-1.15 ± 0.29	38 ± 10	-1.02 ± 0.23	40 ± 12
Apical level	-1.15 ± 0.28	53 ± 8	-1.01 ± 0.19	50 ± 8
Rotational rate (deg s^{-1})				
Basal level	-68.2 ± 23.0	51 ± 12	-56.5 ± 16.8	55 ± 8
Apical level	56.1 ± 20.4	26 ± 10	35.8 ± 15.0**	26 ± 6
Torsional rate (deg s^{-1})	72.3 ± 22.9	49 ± 12	48.5 ± 17.7**	59 ± 17*
Diastole				
Longitudinal SR (s^{-1})	1.55 ± 0.33	138 ± 9	1.38 ± 0.25	138 ± 7
Radial SR (s^{-1})				
Basal level	-1.58 ± 0.35	137 ± 21	-1.33 ± 0.30*	135 ± 26
Apical level	-2.12 ± 0.49	144 ± 13	-1.72 ± 0.59*	150 ± 10
Circumferential SR (s^{-1})				
Basal level	1.25 ± 0.41	129 ± 15	1.14 ± 0.28	132 ± 19
Apical level	1.36 ± 0.29	147 ± 8	1.32 ± 0.29	144 ± 11
Rotational rate (deg.s^{-1})				
Basal level	47.6 ± 15.8	123 ± 24	54.5 ± 23.9	118 ± 17
Apical level	-47.1 ± 29.5	170 ± 11	-44.0 ± 14.0	175 ± 8
Torsional rate (deg s^{-1})	-72.9 ± 20.7	121 ± 14	-68.2 ± 33.5	122 ± 24

SR: Strain rate; Time to peak expressed as percentage of systolic duration. Significantly different from sedentary subjects: *$P < 0.05$, **$P < 0.01$.

level and torsional rate were lower in the cyclists than in controls during systole but not during diastole. LV untwisting during isovolumic relaxation, reached $46 \pm 24\%$ in the cyclists and $44 \pm 22\%$ in controls, respectively (NS). HR correlated with LV torsion ($P < 0.01$) and peak torsion rate during systole ($P < 0.01$) but not during diastole (NS).

Torsion–radial displacement loops (Fig. 5) showed, in both groups, a small initial clockwise twist at the onset of ejection followed by a linearly increasing, counterclockwise twist throughout systole. Torsion and displacement were linearly correlated during systole ($R = 0.94 \pm 0.06$, range: 0.81–0.99 *versus* $R = 0.97 \pm 0.03$, range: 0.81–0.99 in the cyclists and controls, respectively). However, the rate of systolic twist with respect to radial displacement, determined by the slope of systolic twist, was lower in the cyclists than in controls (1.09 ± 0.30 *versus* 1.85 ± 0.60 deg mm^{-1}, respectively, $P < 0.001$), a difference produced by both lower peak torsion (Fig. 4) and higher radial displacement at end-systole (7.5 ± 0.8 mm *versus* 6.4 ± 0.9 mm, respectively, $P < 0.001$). Early diastole was characterized by rapid untwisting despite small radial displacement. From mid to late diastole, untwisting was smaller whereas displacement was larger.

Regional LV rotations and torsion in the subendocardial and subepicardial layers

Mean basal and apical rotations of the subendocardial and subepicardial layers are presented in Table 3. In controls, rotations and torsion were overall higher in the subendocardial than in the subepicardial region. At AVC, differences between the two layers reached statistical significance for basal rotation and for LV torsion, but not for apical rotation. In cyclists, who exhibited lower LV torsion than controls, there were no differences at AVC between subendocardial and subepicardial layers regarding basal and apical rotations as well as torsion. Regional differences in torsion in the six equidistant speckle tracking regions of both layers are depicted in Fig. 6. In both the cyclists and controls, only small differences in subepicardial torsion were found between regions. However, the higher subendocardial torsion in the cyclists than in controls was mainly due to the

higher contribution of the lateral and anterior walls. In both groups, the larger transmural differences in torsion occurred in these two regions, but reached statistical significance only in controls.

Discussion

The aim of the present study was to evaluate LV regional strains in the athlete's heart. We used STI, a new echocardiographic tool, to assess LV normal and shear strains during the cardiac cycle in elite cyclists. The main results were a lower LV apical radial strain and shear strains contrasting with identical LV global systolic and diastolic function. These results emphasize the usefulness of STI to assess regional specificities of the myocardium in the trained heart.

LV systolic strains

Whereas global LV function has been extensively studied (Pluim *et al.* 2000; Fagard, 2003), there have

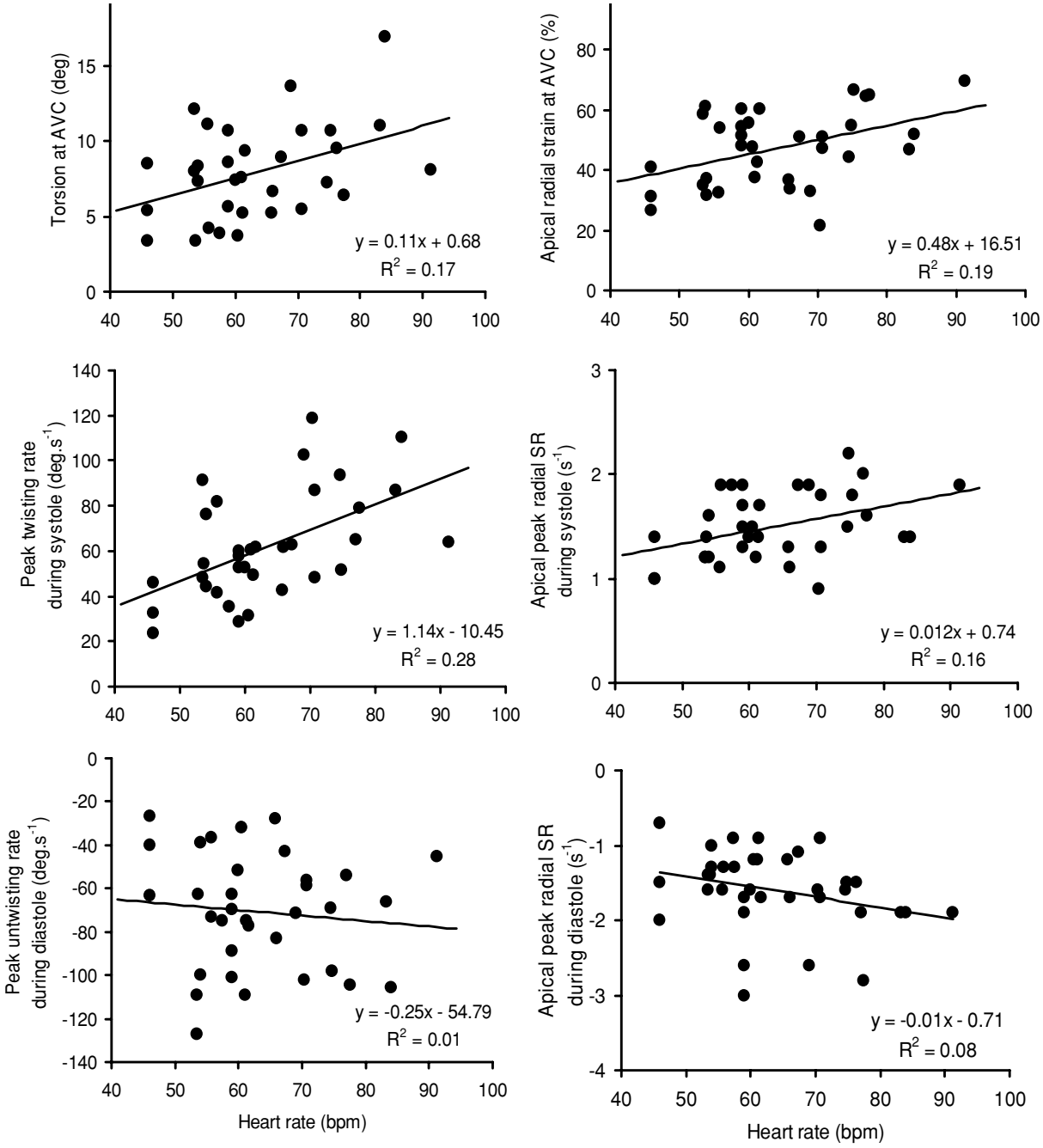

Figure 3. Correlations between heart rate and torsion, torsion rates, radial strain and strain rates

been no reports on regional myocardial strains in endurance-trained subjects. The results of the present study show that long-term high-intensity endurance training induces a non-uniform decrease in the three components of LV normal strains (i.e. longitudinal, circumferential and radial strains). On average, peak longitudinal strain and SR during systole in the cyclists were similar to those observed in their sedentary controls. This result confirms previous data obtained by tissue Doppler imaging (i.e. longitudinal velocities) in our laboratory (Nottin *et al.* 2004) or by others (Schmidt-Trucksäss *et al.* 2001), and highlights that LV longitudinal function is normal in the athlete's heart at rest. However, the short-axis evaluation highlighted that, whereas peak circumferential shortening was normal on both apical and basal regions, peak radial thickening at

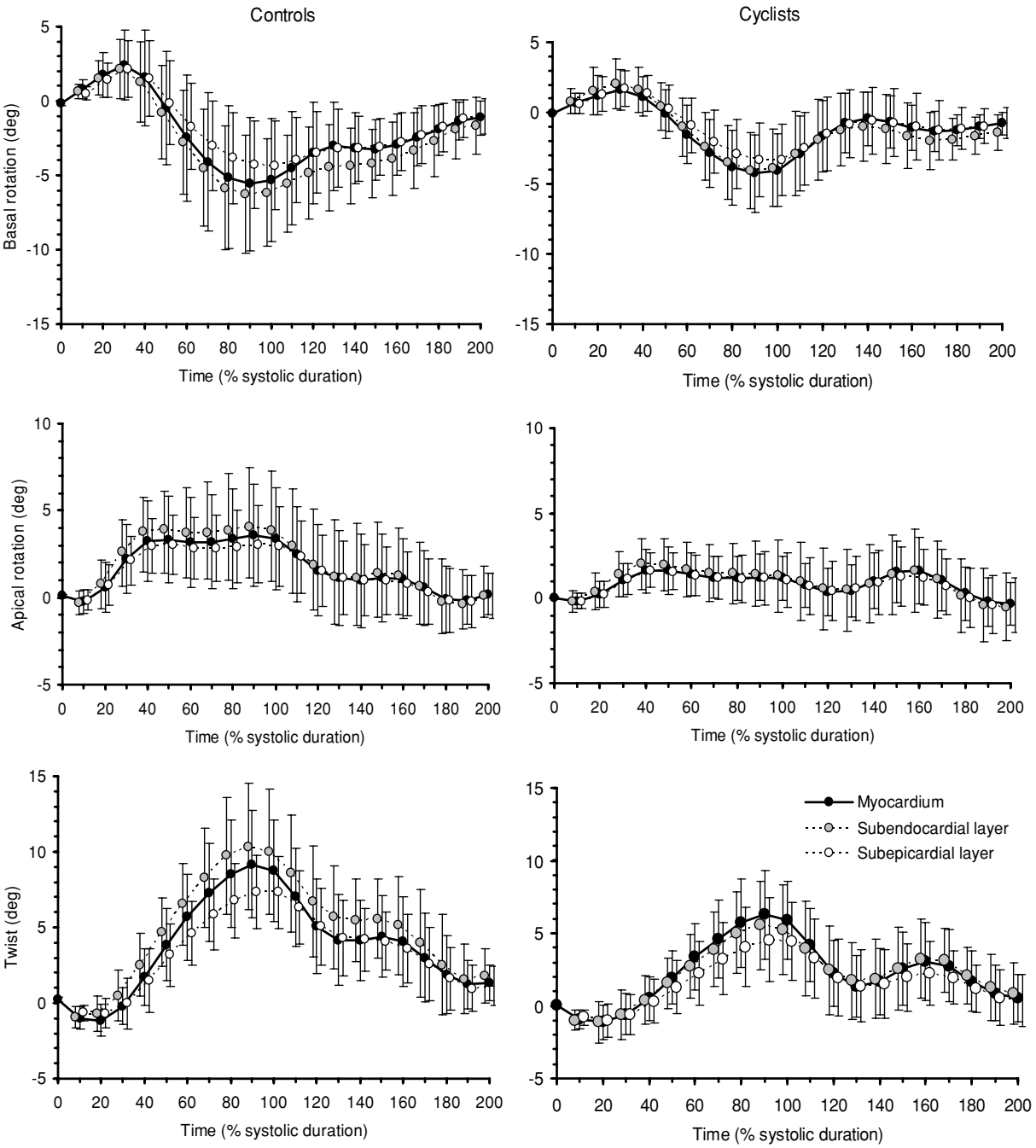

Figure 4. LV basal and apical rotation and LV twist of the subendocardial and subepicardial layers in sedentary subjects (left) and cyclists (right)

Table 3. Peak rotations and torsion of the subendocardial and subepicardial layers

	Controls		Cyclists	
	Subendocardial layer	Subepicardial layer	Subendocardial layer	Subepicardial layer
Basal rotation (deg)	-6.0 ± 3.6	-4.1 ± 3.0†††	-4.5 ± 2.8	-3.6 ± 2.5
Apical rotation (deg)	4.0 ± 3.4	3.0 ± 2.3	1.3 ± 2.1*	1.2 ± 1.5**
Torsion (deg)	10.0 ± 4.3	7.3 ± 2.4†††	5.8 ± 3.1***	4.7 ± 2.6**

Significantly different from sedentary subjects: *$P < 0.05$, **$P < 0.01$, ***$P < 0.001$. Significantly different from subendocardial layer: †††$P < 0.001$.

the apical level was significantly lower in the cyclists when compared to controls. The underlying mechanisms responsible for this still remain partly understood. Recently, Akagawa *et al.* (2007) assessed the effect of sympathetic stimulation on LV radial strains. Interestingly, radial strain increased as dobutamine doses increased along the whole dose range at the apex, but only for low concentrations at the base. This demonstrates that LV radial strain at the apex is more sensitive and dependent on sympathetic stimulation than at the base. Of note, our cyclists had a significantly lower resting HR than controls, which is largely documented in the scientific literature and attributed to training-induced changes in sympathovagal balance, including a decrease in sympathetic activity and a relatively enhanced parasympathetic stimulation (Aubert *et al.* 2003). A decrease in autonomic efferent activity may therefore be involved in the decreased apical radial strains in our cyclists. The significant correlation observed between HR and apical radial strain in the present study speaks in favour of this hypothesis.

Due to the various orientations of myofibres across the LV wall (i.e. subendocardial *versus* subepicardial layers), contraction of myocardium induces shear strains. In the present study, we evaluated LV torsion that resulted from the circumferential–longitudinal component of myocardial shear strains. Moreover, we differentiated between torsion of the inner and outer layers of the myocardium in order to evaluate the circumferential–radial component of myocardial shear strains (Buchalter *et al.* 1990; Hui *et al.* 2007). Our findings emphasized that both components of shear strains were significantly lowered in the athlete's heart at rest. Our regional evaluation highlighted that LV torsion was lower in the cyclists than in controls, especially in the subendocardial layer of the lateral and anterior walls (Fig. 6). The underlying mechanisms responsible for this training-induced decrease in LV shear strains at rest remain unclear. It has been shown that LV torsion depends on the LV wall thickness to LV radius ratio (Lumens *et al.* 2006). However, our cyclists' hypertrophied hearts were characterized by a normal LV wall thickness to radius ratio. MacGowan *et al.* (1996) reported that LV torsion depends also in part on afterload. We calculated systemic vascular resistances, an overall index of afterload, and found no difference between the cyclists and controls. Another plausible explanation for the lower LV torsion observed in the cyclists could be a specific endocardial adaptation to training. Due to their helical pathways with mutually opposite pitch direction, the fibres in the inner and outer layers of the ventricle wall exert opposite torques. Outer layers produce larger torques than inner layers because of their longer lever, resulting in a torsion

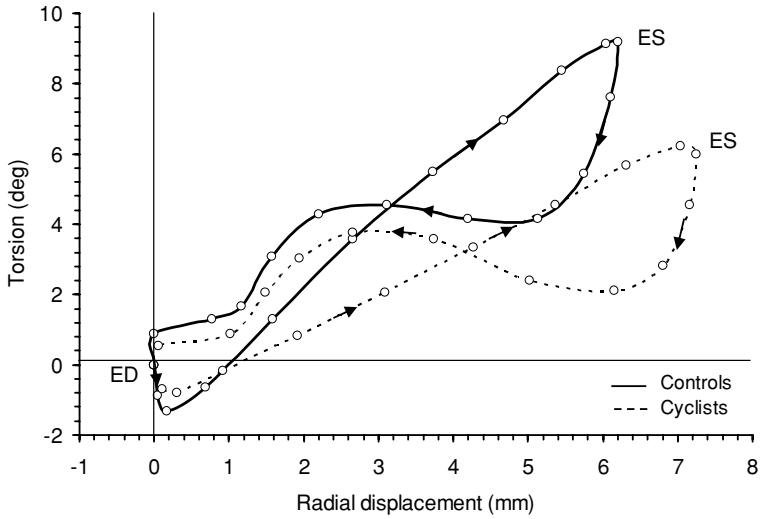

Figure 5. Torsion–radial displacement loops

that favours outer layers. LV torsion increases when subendocardial contractility diminishes, as in patients with aortic stenosis (Van Der Toorn *et al.* 2002), subendocardial infarction (Maruo *et al.* 2007) or with advanced age (Lumens *et al.* 2006; Takeuchi *et al.* 2006). To date there is a distinct lack of data as regards the specific effect of endurance training on subendocardial and subepicardial contractile function. Interestingly, previous animal studies conducted in our laboratory (Cazorla *et al.* 2006) or by others (Diffee & Nagle, 2003) on isolated cardiomyocytes demonstrated that the effect of exercise training on contractile properties was more pronounced in the subendocardial than in the subepicardial region. This regional training-induced adaptation, if present in humans, could constitute a potential mechanism involved in the lower LV torsion observed in our cyclists. This hypothesis needs further investigation to be confirmed. Finally, it has likewise been shown that LV torsion is partly driven by sympathetic activity (Rademakers *et al.* 1992; Akagawa *et al.* 2007; Notomi *et al.* 2006; Notomi *et al.* 2008). The aforementioned reduced sympathetic stimulation at rest in our cyclists might therefore have also contributed to their lower LV torsion.

LV diastolic function

In healthy adults, a MRI evaluation of the time sequence of LV strain development showed that myocardial shear strains resulting from the unfolding of myofibres occur early in diastole (Rosen *et al.* 2004) and are critical in the rapid decrease in LV pressure inducing early filling (Rademakers *et al.* 1992; Notomi *et al.* 2006; Notomi *et al.* 2008). In the present study, despite a decrease in LV shear strains, global diastolic function, assessed by the pattern of LV filling throughout the mitral valve, remained unchanged in the cyclists. We referred to peak longitudinal SR_{IVR} (Wang *et al.* 2007) and peak untwist rate in the early diastole (Notomi *et al.* 2006), as new less load-dependent indexes of LV diastolic function. In our elite cyclists, both indexes of global LV relaxation remained in the same range as those of their sedentary controls, further supporting the notion of normal LV global function at rest in the athlete's heart. Moreover, the twist-displacement loops highlighted that, in both groups, substantial untwisting occurred despite a relatively small radial displacement, in early diastole, whereas untwisting was markedly smaller during the late phases of diastole in spite of substantial radial displacement. This highlights the fact that, in cyclists as well as in controls, the ventricle untwists, rapidly recoiling and creating diastolic suction (Notomi *et al.* 2008). However, since LV shear strains and consequently elastic recoil were lower in the cyclists, other factors such as improved enhanced calcium reuptake by the sarcoplasmic reticulum, *via* an increase in sarcoplasmic reticulum Ca^{2+}-ATPase activity during diastole (Morán *et al.* 2003) might well be involved to allow the cyclists to maintain their LV global diastolic function during resting conditions.

Functional implications

Notomi *et al.* (2006) recently used the concept of LV systolic torsion and subsequent diastolic untwisting to explore the mechanisms of diastolic filling during exercise. They observed that the magnitude of increase in twisting and untwisting rates during exercise was significantly greater than the corresponding changes in LV length and radius. This finding suggests that the enhanced diastolic function during exercise is mainly due to the more vigorous untwisting motion of the LV, especially at the apical level, which induces an increase in intraventricular pressure gradient and thus LV suction. In the present study,

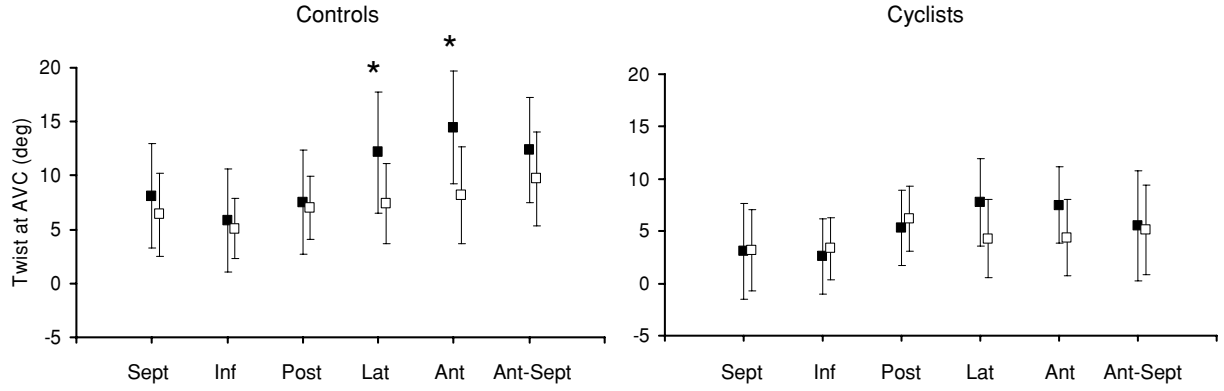

Figure 6. Regional LV twist at aortic valve closure of the subendocardial (filled boxes) and subepicardial (open boxes) layers in sedentary subjects (left) and cyclists (right)
AVC: aortic valve closure; Sept: septal; Inf: inferior; Post: posterior; Lat: lateral; Ant: anterior; Ant-Sept antero-septal.

despite lower LV apical strains and LV shear strains in the cyclists than in controls, overall systolic and diastolic functions were similar. We can reasonably hypothesize that the reduced shear strains observed at rest in the cyclists could represent a greater reserve of shear strains during exercise. In the athlete's heart, this greater reserve could constitute a mechanism by which endurance-trained subjects enhanced their diastolic function during upright exercise compared to sedentary subjects (Matsuda *et al.* 1983; Di Bello *et al.* 1996). This may be a key factor in their greater increase in stroke volume and cardiac performance.

Study limitations and future research

This study suffers from some limitations. Since a cross-sectional study is by nature descriptive, further studies including training programmes will be needed to ascertain that differences in LV normal and shear strains reported here are effectively linked to training stimuli. We did not use any gold standard to measure LV torsion. The exact location of the basal and apical planes may be different from patient to patient, resulting in some measurement errors. However, a previous study has recently validated the accuracy of STI *versus* tagged MRI (Helle-Valle *et al.* 2005). On the other hand, STI analysis cannot eliminate errors introduced by through-plane motion, particularly at the basal level. For the assessment of circumferential-radial shear strains, we used an index based on the intramural differences in LV torsion. This method requires the ROI corresponding to the sub-epicardium and subendocardium layers to be determined subjectively. Future experiments using 3D tagged MRI, which is to date considered as the gold standard method to evaluate shear strains inside the myocardium, might resolve this issue.

The results of the present experiment raised a number of important questions. One potential mechanism for the reduced LV strains and torsion observed in our athletes could be their reduced sympathetic stimulation during resting conditions, and further studies using dobutamine stress echocardiography will be needed to test this assumption. Another plausible explanation is related to a specific effect of endurance training on subendocardial and subepicardial contractile function. Further experiments using animal models will have to be carried out to check this hypothesis and, if this effect is confirmed, to better understand the underlying mechanisms responsible for such regional adaptations. Finally, patterns of LV normal and shear strains should be evaluated during effort to see whether the alterations observed in the present study at rest have functional significance during exercise.

Conclusion

STI allowed the assessment of LV normal and shear strains in elite endurance cyclists and sedentary controls. The athlete's heart was characterized by specific adaptations including lower LV apical radial strain and shear strains. These physiological adaptations observed during resting conditions raised some questions. Further studies are needed to evaluate their role in the enhanced cardiac performance observed during exercise in highly trained athletes.

References

Akagawa E, Murata K, Tanaka N, Yamada H, Miura T, Kunichika H, Wada Y, Hadano Y, Tanaka T, Nose Y, Yasumoto K, Kono M & Matsuzaki M (2007). Augmentation of left ventricular apical endocardial rotation with inotropic stimulation contributes to increased left ventricular torsion and radial strain in normal subjects: quantitative assessment utilizing a novel automated tissue tracking technique. *Circ J* **71**, 661–668.

Amundsen BH, Helle-Valle T, Edvardsen T, Torp H, Crosby J, Lyseggen E, Støylen A, Ihlen H, Lima JA, Smiseth OA & Slørdahl SA (2006). Noninvasive myocardial strain measurement by speckle tracking echocardiography: validation against sonomicrometry and tagged magnetic resonance imaging. *J Am Coll Cardiol* **47**, 789–793.

Aubert AE, Seps B & Beckers F (2003). Heart rate variability in athletes. *Sports Med* **33**, 889–919.

Buchalter MB, Weiss JL, Rogers WJ, Zerhouni EA, Weisfeldt ML, Beyar R & Shapiro EP (1990). Noninvasive quantification of left ventricular rotational deformation in normal humans using magnetic resonance imaging myocardial tagging. *Circulation* **81**, 1236–1244.

Caso P, D'Andrea A, Galderisi M, Liccardo B, Severino S, De Simone L, Izzo A, D'Andrea L & Mininni N (2000). Pulsed Doppler tissue imaging in endurance athletes: relation between left ventricular preload and myocardial regional diastolic function. *Am J Cardiol* **85**, 1131–1136.

Cazorla O, Aït Mou Y, Goret L, Vassort G, Dauzat M, Lacampagne A, Tanguy S & Obert P (2006). Effects of high-altitude exercise training on contractile function of rat skinned cardiomyocyte. *Cardiovasc Res* **71**, 652–660.

Devereux RB, Alonso DR, Lutas EM, Gottlieb GJ, Campo E, Sachs I & Reichek N (1986). Echocardiographic assessment of left ventricular hypertrophy: comparison to necropsy findings. *Am J Cardiol* **57**, 450–458.

Di Bello V, Santoro G, Talarico L, Di Muro C, Caputo MT, Giorgi D, Bertini A, Bianchi M & Giusti C (1996). Left ventricular function during exercise in athletes and in sedentary men. *Med Sci Sports Exerc* **28**, 190–196.

Diffee GM & Nagle DF (2003). Regional differences in effects of exercise training on contractile and biochemical properties of rat cardiac myocytes. *J Appl Physiol* **95**, 35–42.

Dong SJ, Hees PS, Siu CO, Weiss JL & Shapiro EP (2001). MRI assessment of LV relaxation by untwisting rate: a new isovolumic phase measure of tau. *Am J Physiol Heart Circ Physiol* **281**, H2002–H2009.

Durnin JV & Rahaman MM (1967). The assessment of the amount of fat in the human body from measurements of skinfold thickness. *Br J Nutr* **21**, 681–689.

Fagard R (2003). Athlete's heart. *Heart* **89**, 1455–1461.

Greenbaum RA, Ho SY, Gibson DG, Becker AE & Anderson RH (1981). Left ventricular fibre architecture in man. *Br Heart J* **45**, 248–263.

Hashimoto I, Li XK, Bhat AH, Jones M & Sahn DJ (2005). Quantitative assessment of regional peak myocardial acceleration during isovolumic contraction and relaxation times by tissue Doppler imaging. *Heart* **91**, 811–816.

Helle-Valle T, Crosby J, Edvardsen T, Lyseggen E, Amundsen BH, Smith HJ, Rosen BD, Lima JA, Torp H, Ihlen H & Smiseth OA (2005). New noninvasive method for assessment of left ventricular rotation: speckle tracking echocardiography. *Circulation* **112**, 3149–3156.

Hui L, Pemberton J, Hickey E, Li XK, Lysyansky P, Ashraf M, Niemann PS & Sahn DJ (2007). The contribution of left ventricular muscle bands to left ventricular rotation: assessment by a 2-dimensional speckle tracking method. *J Am Soc Echocardiogr* **20**, 486–491.

Leitman M, Lysyansky P, Sidenko S, Shir V, Peleg E, Binenbaum M, Kaluski E, Krakover R & Vered Z (2004). Two-dimensional strain – a novel software for real-time quantitative echocardiographic assessment of myocardial function. *J Am Soc Echocardiogr* **17**, 1021–1029.

Lumens J, Delhaas T, Arts T, Cowan BR & Young AA (2006). Impaired subendocardial contractile myofibre function in asymptomatic aged humans, as detected using MRI. *Am J Physiol Heart Circ Physiol* **291**, H1573–H1579.

MacGowan GA, Burkhoff D, Rogers WJ, Salvador D, Azhari H, Hees PS, Zweier JL, Halperin HR, Siu CO, Lima JA, Weiss JL & Shapiro EP (1996). Effects of afterload on regional left ventricular torsion. *Cardiovasc Res* **31**, 917–925.

Maruo T, Nakatani S, Jin Y, Uemura K, Sugimachi M, Ueda-Ishibashi H, Kitakaze M, Ohe T, Sunagawa K & Miyatake K (2007). Evaluation of transmural distribution of viable muscle by myocardial strain profile and dobutamine stress echocardiography. *Am J Physiol Heart Circ Physiol* **292**, H921–H927.

Matsuda M, Sugishita Y, Koseki S, Ito I, Akatsuka T & Takamatsu K (1983). Effect of exercise on left ventricular diastolic filling in athletes and nonathletes. *J Appl Physiol* **55**, 323–328.

Moon MR, Ingels NB, Jr Daughters GT 2nd, Stinson EB, Hansen DE & Miller DC (1994). Alterations in left ventricular twist mechanics with inotropic stimulation and volume loading in human subjects. *Circulation* **89**, 142–150.

Moore CC, McVeigh ER & Zerhouni EA (2000). Quantitative tagged magnetic resonance imaging of the normal human left ventricle. *Top Magn Reson Imaging* **11**, 359–371.

Morán M, Saborido A & Megías A (2003). Ca^{2+} regulatory systems in rat myocardium are altered by 24 weeks treadmill training. *Pflugers Arch* **446**, 161–168.

Nagueh SF, Middleton KJ, Kopelen HA, Zoghbi WA & Quiñones MA (1997). Doppler tissue imaging: a noninvasive technique for evaluation of left ventricular relaxation and estimation of filling pressures. *J Am Coll Cardiol* **30**, 1527–1533.

Nakai H, Takeuchi M, Nishikage T, Kokumai M, Otani S & Lang RM (2006). Effect of aging on twist-displacement loop by 2-dimensional speckle tracking imaging. *J Am Soc Echocardiogr* **19**, 880–885.

Notomi Y, Martin-Miklovic MG, Oryszak SJ, Shiota T, Deserranno D, Popovic ZB, Garcia MJ, Greenberg NL & Thomas JD (2006). Enhanced ventricular untwisting during exercise: a mechanistic manifestation of elastic recoil described by Doppler tissue imaging. *Circulation* **113**, 2524–2533.

Notomi Y, Popovic ZB, Yamada H, Wallick DW, Martin MG, Oryszak SJ, Shiota T, Greenberg NL & Thomas JD (2008). Ventricular untwisting: a temporal link between left ventricular relaxation and suction. *Am J Physiol Heart Circ Physiol* **294**, H505–H513.

Nottin S, Nguyen LD, Terbah M & Obert P (2004). Left ventricular function in endurance-trained children by tissue Doppler imaging. *Med Sci Sports Exerc* **36**, 1507–1513.

Pelliccia A, Maron BJ, Spataro A, Proschan MA & Spirito P (1991). The upper limit of physiologic cardiac hypertrophy in highly trained elite athletes. *N Engl J Med* **324**, 295–301.

Pluim BM, Zwinderman AH, van der Laarse A & Van der Wall EE (2000). The athlete's heart. A meta-analysis of cardiac structure and function. *Circulation* **101**, 336–344.

Rademakers FE, Buchalter MB, Rogers WJ, Zerhouni EA, Weisfeldt ML, Weiss JL & Shapiro EP (1992). Dissociation between left ventricular untwisting and filling. Accentuation by catecholamines. *Circulation* **85**, 1572–1581.

Rosen BD, Gerber BL, Edvardsen T, Castillo E, Amado LC, Nasir K, Kraitchman DL, Osman NF, Bluemke DA & Lima JA (2004). Late systolic onset of regional LV relaxation demonstrated in three-dimensional space by MRI tissue tagging. *Am J Physiol Heart Circ Physiol* **287**, H1740–H1746.

Saghir M, Areces M & Makan M (2007). Strain rate imaging differentiates hypertensive cardiac hypertrophy from physiologic cardiac hypertrophy (athlete's heart). *J Am Soc Echocardiogr* **20**, 151–157.

Sahn DJ, DeMaria A, Kisslo J & Weyman A (1978). Recommendations regarding quantitation in M-mode echocardiography: results of a survey of echocardiographic measurements. *Circulation* **58**, 1072–1083.

Schmidt-Trucksäss A, Schmid A, Häussler C, Huber G, Huonker M & Keul J (2001). Left ventricular wall motion during diastolic filling in endurance-trained athletes. *Med Sci Sports Exerc* **33**, 189–195.

Takeuchi M, Nakai H, Kokumai M, Nishikage T, Otani S & Lang RM (2006). Age-related changes in left ventricular twist assessed by two-dimensional speckle-tracking imaging. *J Am Soc Echocardiogr* **19**, 1077–1084.

Torrent-Guasp F, Buckberg GD, Clemente C, Cox JL, Coghlan HC & Gharib M (2001). The structure and function of the helical heart and its buttress wrapping. I. The normal macroscopic structure of the heart. *Semin Thorac Cardiovasc Surg* **13**, 301–319.

Van der Toorn A, Barenbrug P, Snoep G, Van der Veen FH, Delhaas T, Prinzen FW, Maessen J & Arts T (2002). Transmural gradients of cardiac myofibre shortening in aortic valve stenosis patients using MRI tagging. *Am J Physiol Heart Circ Physiol* **283**, H1609–H1615.

Wang J, Khoury DS, Thohan V, Torre-Amione G & Nagueh SF (2007). Global diastolic strain rate for the assessment of left ventricular relaxation and filling pressures. *Circulation* **115**, 1376–1383.

Acknowledgements

We thank GE Medical Systems–Ultrasound France for providing the ultrasonic equipment used for this study. The authors affirm that they have no personal interest, financial or otherwise, with any commercial company with potential financial interest in the subject matter enclosed in this article.